

<sup>1</sup> Loránd Eötvös University, Budapest, Hungary

<sup>2</sup> Wigner Research Centre for Physics, Hungarian Academy of Sciences, Budapest, Hungary

<sup>3</sup> Department of Physics, Western Michigan University, Kalamazoo, USA

## 1. Motivation: Laser physics and non-linear QED

Pair production from vacuum has long been predicted in QED. However the threshold field is extremely high:

$$E_{critical} = \frac{m^2 c^3}{q\hbar} \approx 1.3 \cdot 10^{18} \frac{V}{m} \approx 10^{30} \frac{W}{cm^2}$$

in pure static and homogeneous electric fields. Recent calculations suggest that special time dependences can significantly lower this threshold. With the rapid development of laser technology the experimental observation of vacuum pair production seems to be possible in the near future. This will open a new area for research and applications: the non-linear QED regime.

The investigation of realistic field configurations however remains a great challenge both theoretically and computationally.

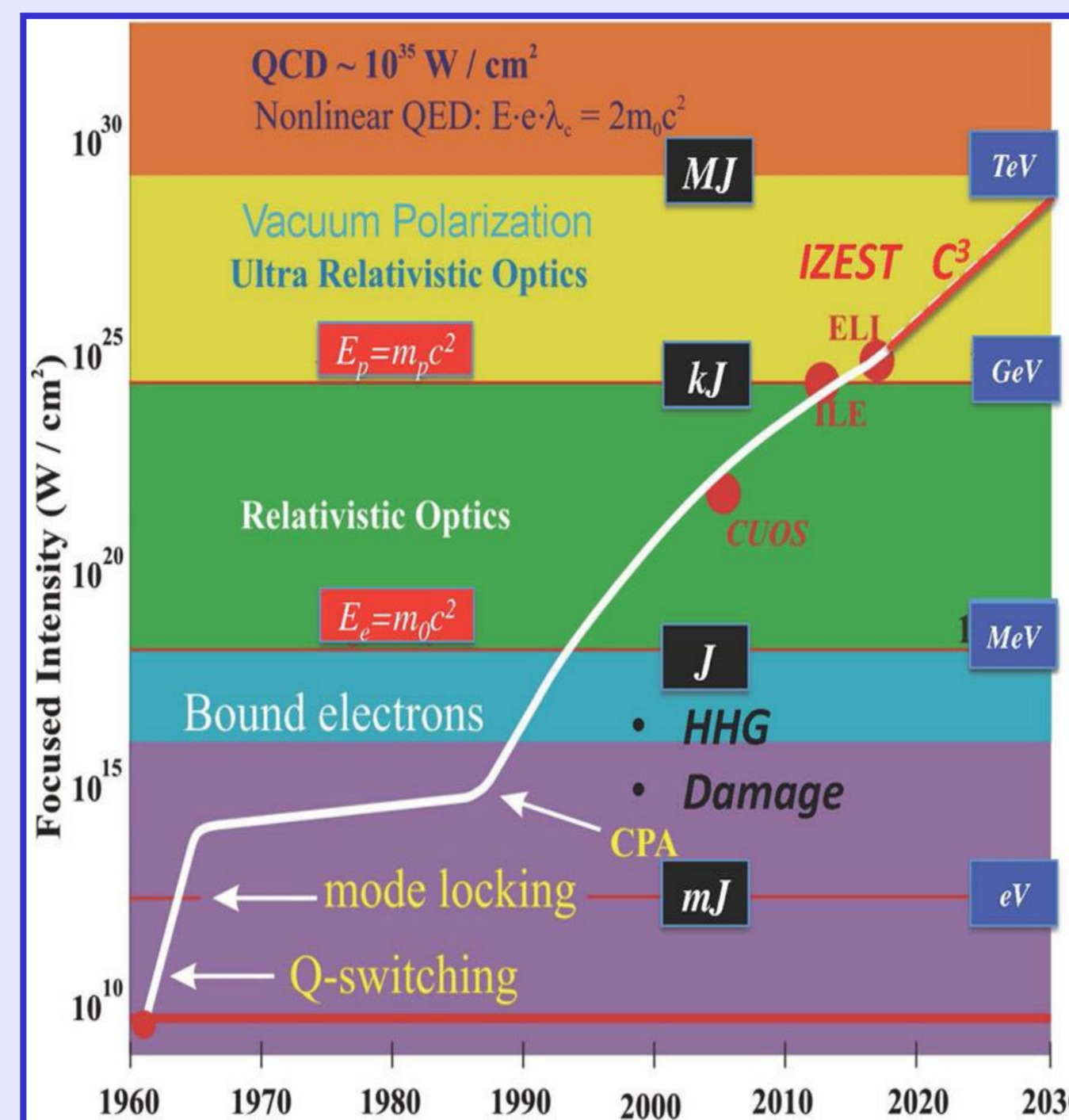


Figure 1.: Experimentally attainable laser intensities. Figure after [1].

## 2. Motivation: Relativistic Heavy Ion Collisions

Pair production can also happen in QCD. In fact the most successful model for the initial stages of heavy ion collisions is based on color strings/ropes that form when quark - anti quarks are separating as the nuclei pass through each other.

Because the gluon field strength grows linearly with distance at some point the field energy exceeds the rest mass of a new quark pair and pair production occurs.

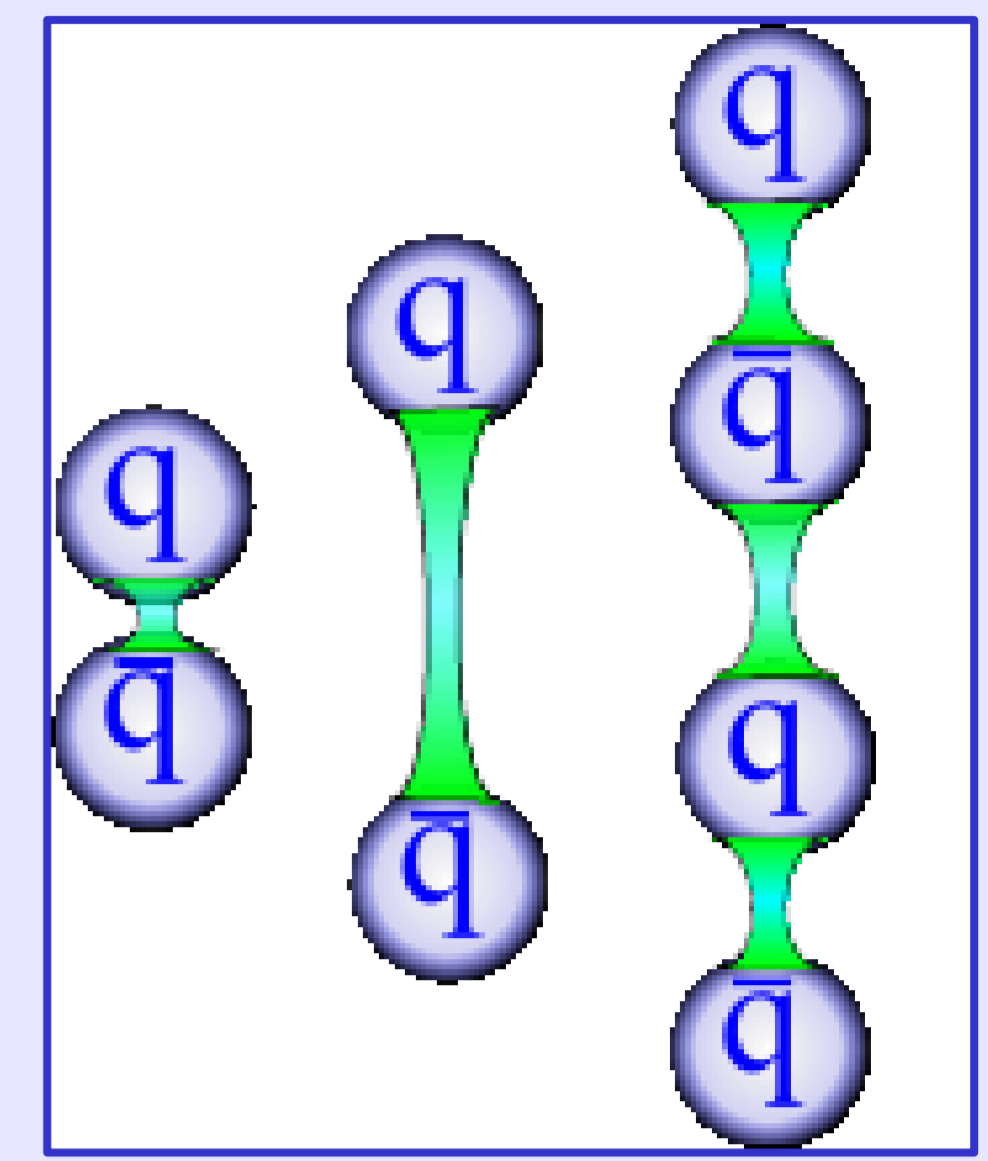


Figure 2.: QCD pair production from the separation of a quark pair.

The identification of this process from experimental data is difficult because thermalization, hydrodynamic evolution and hadronisation may mask the characteristics of pair production.

## 3. Theoretical description: Wigner-functions

Pair production is inherently a quantum phenomena. Wigner-functions provide a natural and easily comprehensible way of representing such a system in phase-space just like ordinary density functions in classical mechanics [2, 3].

The Wigner-functions have the following properties:

- They are real valued and bounded.
- They are not positive semi-definite distributions, because genuine quantum effects are encoded in negative places that vanish in the classical limit.
- Marginal distributions and operator expectation values are obtained as phase-space integrals.
- The time evolution in phase-space is nearly classical.

The relativistic one-particle Wigner-function is defined as:

$$\hat{C}(\vec{x}, \vec{s}, t) = \exp\left(-iq \int_{-1/2}^{1/2} \vec{A}(\vec{x} + \lambda \vec{s}, t) \vec{s} d\lambda\right) \left[ \Psi\left(\vec{x} + \frac{\vec{s}}{2}\right), \bar{\Psi}\left(\vec{x} - \frac{\vec{s}}{2}\right) \right]$$

$$W(\vec{x}, \vec{p}, t) = -\frac{1}{2} \int e^{-i\vec{p}\vec{s}} \langle 0 | \hat{C}(\vec{x}, \vec{s}, t) | 0 \rangle d\vec{s}$$

where  $\vec{A}$  is the vector potential of the QED field.

The time evolution is obtained by taking the time derivative of the Wigner-function and inserting the proper Dirac-equation. At this point the following approximation is used: the fields are extracted as c-number field from the expectation values. This is a tree-level truncation and means that radiative corrections are neglected.

The equation of motion in a compact form is:

$$D_t W = -\frac{1}{2} D_x [\gamma^0 \vec{\gamma}, W] - im [\gamma^0 \vec{\gamma}, W] - iP \{\gamma^0 \vec{\gamma}, W\}$$

After expanding on the Dirac matrix basis we end up at the following evolution equation for the 16 real components of the Wigner-function:

$$\begin{aligned} D_t s - 2\vec{P}\vec{t}_1 &= 0 \\ D_t p + 2\vec{P}\vec{t}_2 &= 2m\mathfrak{a}_0 \\ D_t v_0 + \vec{D}_x \vec{v} &= 0 \\ D_t \mathfrak{a}_0 + \vec{D}_x \vec{\mathfrak{a}} &= 2m\mathfrak{p} \end{aligned}$$

$$\begin{aligned} D_t \vec{v} + \vec{D}_x v_0 + 2\vec{P} \times \vec{\mathfrak{a}} &= -2m\vec{t}_1 \\ D_t \vec{\mathfrak{a}} + \vec{D}_x \mathfrak{a}_0 + 2\vec{P} \times \vec{v} &= 0 \\ D_t \vec{t}_1 + \vec{D}_x \times \vec{t}_2 + 2\vec{P}s &= 2m\vec{v} \\ D_t \vec{t}_2 - \vec{D}_x \times \vec{t}_1 - 2\vec{P}p &= 0 \end{aligned}$$

Where the following non-local operators appeared:

$$\begin{aligned} D_t &= \partial_t + q\vec{E}(\vec{x}, t) \vec{v}_p - \frac{q\hbar^2}{12} (\vec{v}_p \vec{v}_x)^2 \vec{E}(\vec{x}, t) \vec{v}_p + \dots \\ \vec{D}_x &= \vec{v}_x + q\vec{B}(\vec{x}, t) \times \vec{v}_p - \frac{q\hbar^2}{12} (\vec{v}_p \vec{v}_x)^2 \vec{B}(\vec{x}, t) \times \vec{v}_p + \dots \\ \vec{P} &= \vec{p} + \frac{q\hbar}{12} (\vec{v}_p \vec{v}_x) \vec{B}(\vec{x}, t) \times \vec{v}_p + \dots \end{aligned}$$

The Wigner formalism was extended to SU(N) theories and the evolution equations were derived for the general case. Further studies showed that the particle spectras are not that much different from the U(1) QED case: there seems to be a strong Abelian dominance in QCD pair production [4].

Owing to these results we use the QED formalism to study the effect of inhomogeneities on particle production. Since the problem is computationally demanding we restrict the inhomogeneity to 1 space direction and use the following electric field:

$$\vec{E}(\vec{x}, t) = \vec{e}_z E_0 \cosh^{-2}\left(\frac{t}{\tau}\right) \times \frac{1}{2} \left( 1 - \tanh\left(\frac{x+R}{r}\right) \tanh\left(\frac{x-R}{r}\right) \right)$$

This models the cross-section of a color string in one dimension, while the time dependent part is the so-called Sauter field for which an analytical solution of the pair distribution is known. The pair number density is built from the Wigner-function components as:

$$f = \frac{1}{2} + \frac{ms + \vec{p}\vec{v}}{4\sqrt{m^2 + p^2}}$$

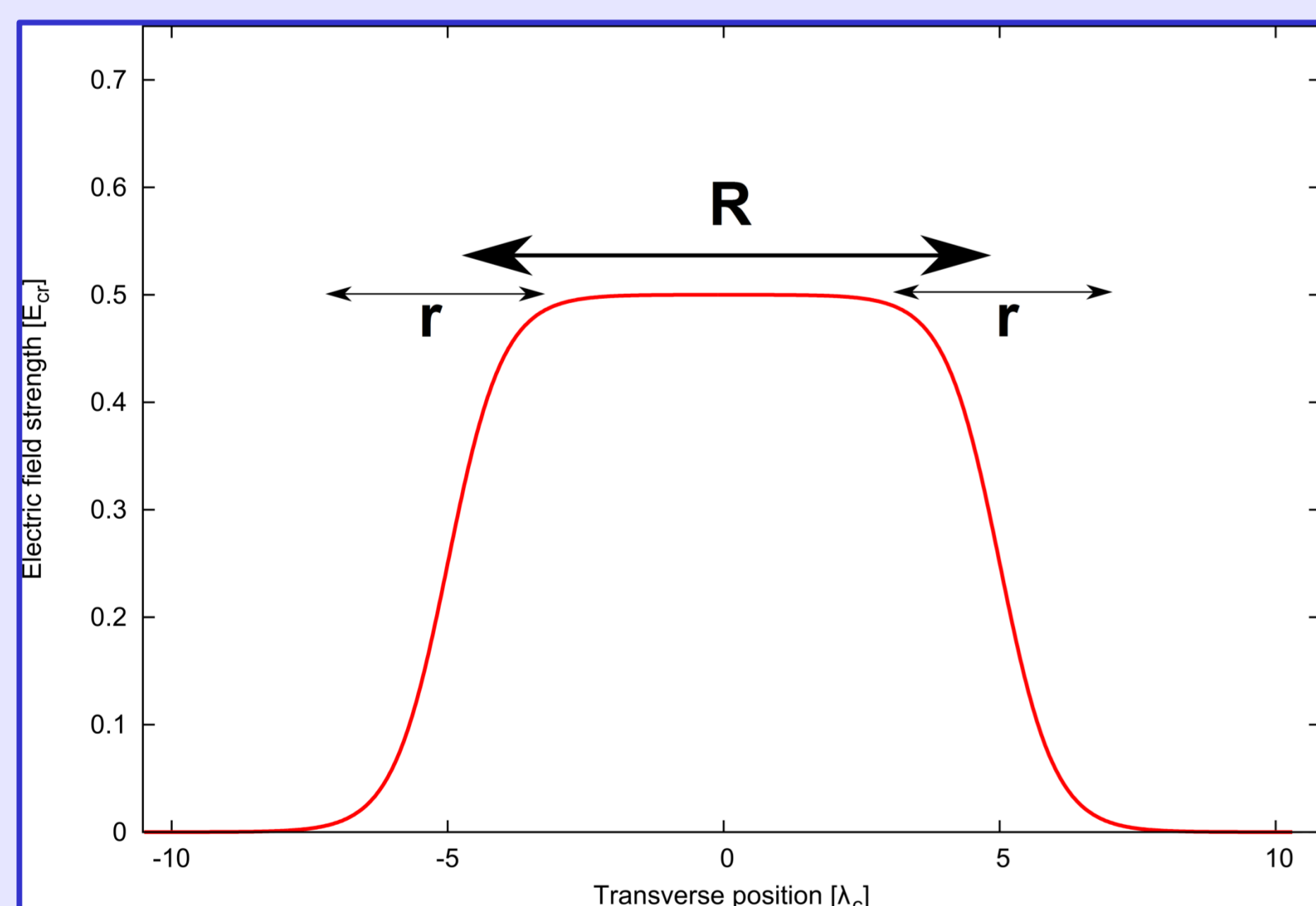


Figure 3.: Model field for the QCD color string.

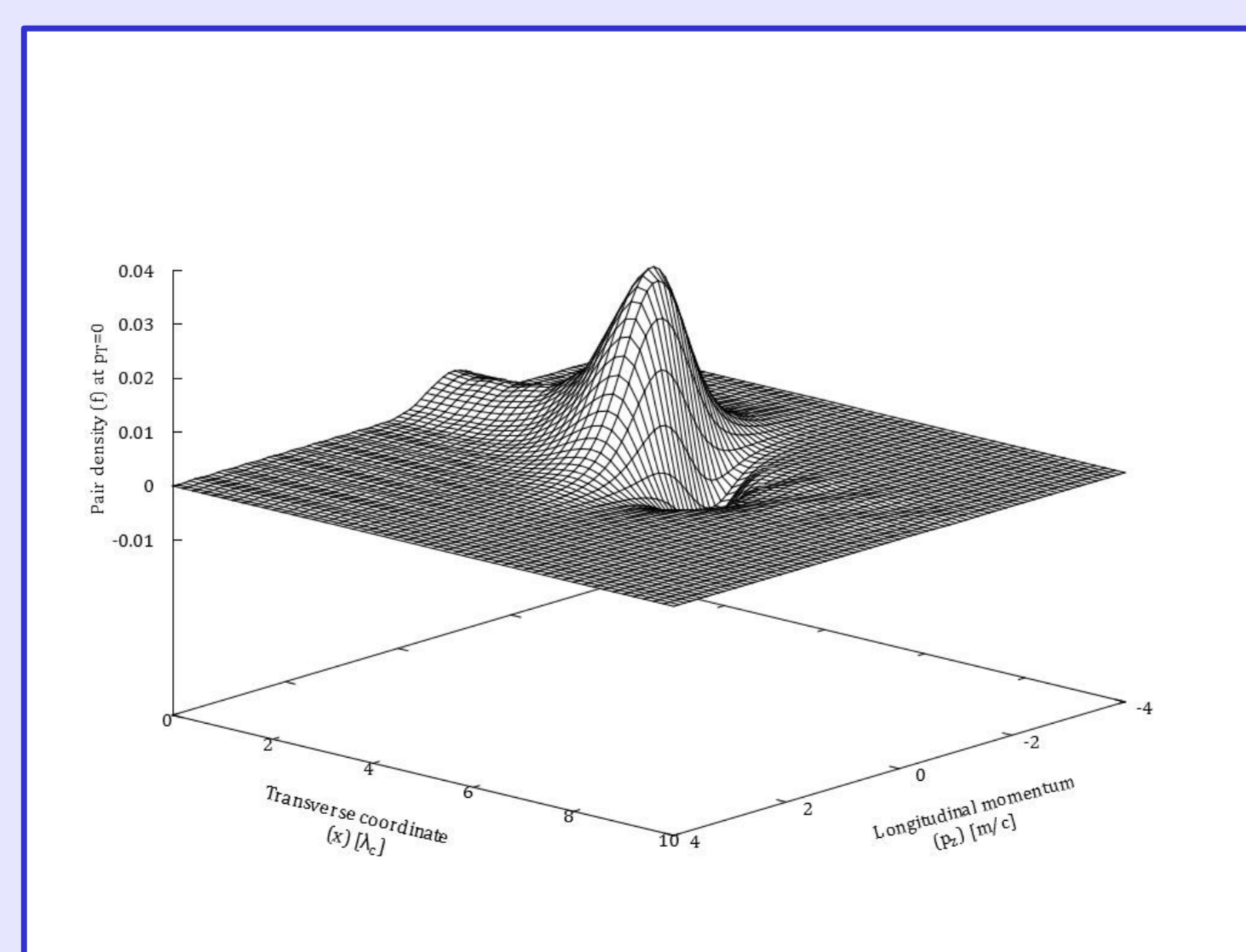


Figure 4.: Asymptotic pair density in the phase-space.

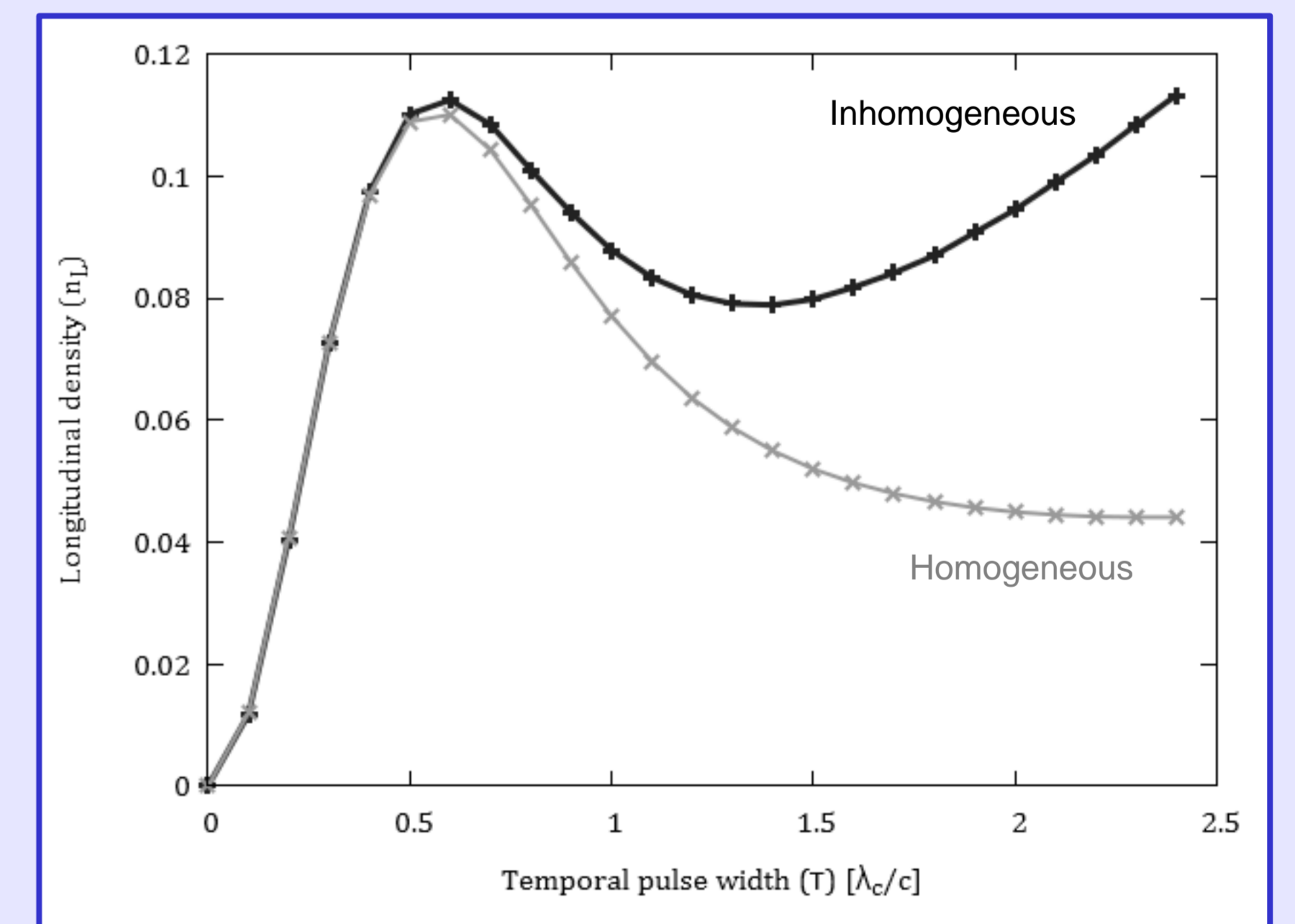


Figure 5.: Pulse width dependence of the integrated pair density.

## 4. Abelian model of pair production from the color string

We solved the 16 component evolution equations for the chosen field numerically. Fig. 4. shows an example of the asymptotic pair density. Note that the peak is precisely where the field gradient is the largest at  $x = 5\lambda_c$ . We performed parameter scans with varying temporal width  $\tau$  and spatial extent  $R$ .

We show the particle density at  $p_T = 0$  with longitudinal momenta and transverse position integrated:

$$n_L = \int_{-\infty}^{\infty} dx \frac{dp_z}{2\pi} f(x, p_T = 0, p_z)$$

and compare the homogeneous and inhomogeneous yields with the same temporal shape.

Fig. 5. shows the temporal scan results. The shorter pulses produce the same number of pairs in the two case, but for longer pulses the inhomogeneous yield is much higher than the homogeneous reference.

Fig. 6. compares the effect of changing the spatial width of the pulse. We find that the slopes of the two cases is the same they only differ in a constant. This together with Fig. 4. suggests that the inhomogeneity effect is a surface effect as predicted by Heisenberg in 1934 [5]. These results suggest that the widely used homogeneous string models may underestimate yields and miss important features.

### References:

- [1] T. Tajima, G. Mourou, Phys. Rev. ST. Vol 5. 031301 (2002)
- [2] I. Bialynicki-Birula, P. Gornicki, J. Rafelski, Phys. Rev. D44, 1825-1835. (1991)
- [3] F. Hebenstreit, R. Alkofer, H. Gies, Phys. Rev. D82 105026. (2010)
- [4] V. V. Skokov and P. Levai, Phys. Rev. D78, 054004. (2008)
- [5] W. Heisenberg, Sachsische Akademie der Wissenschaften, 86, 317. (1934)

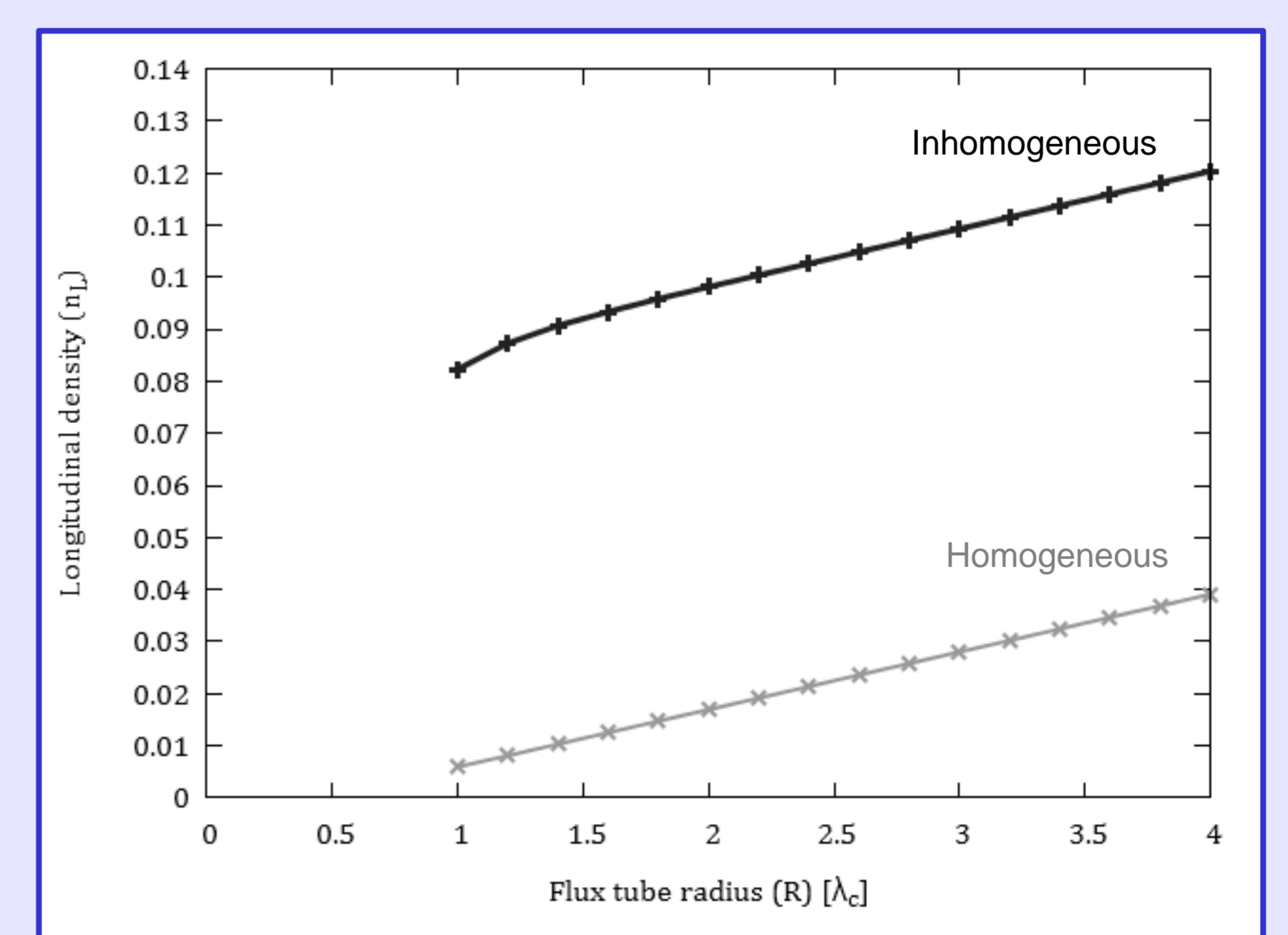


Figure 6.: Pair production rate scaling with increasing flux tube radius. Note the same slope.